Primordial magnetism in CMB polarization

Levon Pogosian

Department of Physics, Simon Fraser University, Burnaby, BC, V5A 1S6, Canada

E-mail: `levon@sfu.ca`

Abstract. A large scale B-mode signal in the CMB polarization would constitute a smoking gun of Inflation and is the main target of several ongoing and upcoming experiments. In this contribution, I consider distinguishing features of another potential source of primordial B-modes – magnetic fields. In particular, the Faraday Rotation of CMB polarization provides a distinctive signature of cosmic magnetic fields through the characteristic frequency dependence and the mode-coupling correlations of the CMB variables. I discuss constraints on primordial magnetism that can be expected from future CMB experiments, taking into account the obstruction caused by the magnetic field of the Milky Way.

1. Introduction

The unexplained origin of the galactic and extragalactic magnetic fields is one of the long standing problems of cosmology and astrophysics. While in the case of mature galaxies magnetic fields perhaps could be generated through a dynamo mechanism [1], explaining their presence in young protogalaxies and, possibly, in the intergalactic space [2], is more challenging. It is possible that there is yet unknown astrophysical mechanism that can generate magnetic fields on large scales and high redshifts. Another possibility is that magnetic fields existed before astrophysical structures began to form [3]. A primordial magnetic field (PMF) could be produced in the aftermath of cosmic phase transitions [4, 5] or in specially designed inflationary scenarios [6, 7]. Measurements of cosmic microwave background (CMB) temperature and polarization could decisively prove their primordial origin if they contained magnetic signatures present at the time of last scattering. A discovery of PMF would have profound implications for our understanding of the early universe, with critical insights into fundamental problems such as the matter-antimatter asymmetry [8].

A stochastic PMF influences CMB observables in several ways. Magnetic stress-energy perturbs the metric which leads to CMB anisotropies, while the Lorentz force deflects moving electrons and protons coupled to photons. Recently, it has been suggested [9] that small-scale fields can appreciably alter the recombination history and, consequently, the distance to last scattering, because of the enhanced small scale baryonic inhomogeneities. Here we focus on another signature of PMF – the Faraday Rotation (FR) of CMB polarization.

FR produces a B mode type polarization with a characteristic spectrum [10, 11] as well as non-trivial 4-point correlations of the CMB temperature and polarization. In [12, 13, 14], we examined detectability of PMF using different correlators and evaluated their relative merits. We found that a Planck-like experiment can detect scale-invariant PMF of a several nano-Gauss (nG) strength using the FR diagnostic, while realistic future experiments at the same frequency

can detect 10^{-10} Gauss. This is comparable or better than other CMB probes of PMF, and using multiple frequency channels can further improve on these prospects [14].

2. B-modes from Faraday Rotation

At a given direction $\hat{\mathbf{n}}$ on the sky, CMB is characterized by its intensity and two additional Stokes parameters, Q and U, quantifying its linear polarization. While $Q(\hat{\mathbf{n}})$ and $U(\hat{\mathbf{n}})$ are the quantities that experiments directly measure, their values depend on the choice of the coordinate axes. Instead, it has become customary to interpret polarization maps by separating them into parity-even and parity-odd patterns, or the so-called E and B modes [15, 16]. Existence of intensity fluctuations at last scattering implies generation of E modes, which by now have been observed and found to be consistent with the spectrum of temperature anisotropies. On the other hand, B modes would not be generated at last scattering unless there were gravitational waves or other sources of metric perturbations with parity-odd components such as cosmic defects [17] or magnetic fields [18]. Weak lensing (WL) of CMB photons by the large scale structures along the line of sight distorts polarization patterns generated at last scattering and converts some of the E mode into B modes, which is expected to be measured with upcoming CMB experiments.

A primordial magnetic field present at and just after last scattering will Faraday-rotate the plane of polarization of the CMB photons. The rotation angle along $\hat{\mathbf{n}}$ is given by

$$\alpha(\hat{\mathbf{n}}) = \frac{3}{16\pi^2 e}\lambda_0^2 \int \dot{\tau}\, \mathbf{B} \cdot d\mathbf{l} \,, \tag{1}$$

where $\dot{\tau} \equiv n_e \sigma_T a$ is the differential optical depth, n_e is the line of sight free electron density, σ_T is the Thomson scattering cross-section, a is the scale factor, λ_0 is the observed wavelength of the radiation, $\mathbf{B}$ is the "comoving" magnetic field, and $d\mathbf{l}$ is the comoving length element along the photon trajectory.

A statistically homogeneous, isotropic and Gaussian distributed stochastic magnetic field can be characterized by a two-point correlation function in Fourier space

$$\langle b_i(\mathbf{k})b_j(\mathbf{k}')\rangle = (2\pi)^3 \delta^{(3)}(\mathbf{k} + \mathbf{k}')[(\delta_{ij} - \hat{k}_i\hat{k}_j)S(k) \tag{2}$$

where $S(k)$ is the symmetric magnetic power spectrum, and where we omit the anti-symmetric contribution that quantifies the amount of magnetic helicity because only $S(k)$ contributes to the CMB observables evaluated in this paper. The shape of $S(k)$ depends on the mechanism responsible for production of PMF and generally can be taken to be a power law up to a certain dissipation scale, $S(k) \propto k^{2n-3}$ for $0 < k < k_{\text{diss}}$, and zero at higher k. The dissipation scale, k_{diss}, should, in principle, be dependent on the amplitude and the shape of the magnetic fields spectrum. We assume that k_{diss} is determined by damping into Alfven waves [19, 20] and can be related to B_{eff} as

$$\frac{k_{\text{diss}}}{1\text{Mpc}^{-1}} \approx 1.4\, h^{1/2}\left(\frac{10^{-7}\text{Gauss}}{B_{\text{eff}}}\right) \,, \tag{3}$$

where B_{eff} is defined as the effective homogeneous field strength that would have the same total magnetic energy density. B_{eff} is related to the fraction of magnetic energy density to the total radiation density, $\Omega_{B\gamma}$, via [11]

$$B_{\text{eff}} = 3.25 \times 10^{-6}\sqrt{\Omega_{B\gamma}}\ \text{Gauss} \,. \tag{4}$$

The generation of CMB polarization and the FR happen concurrently during the epoch of last scattering. However, as we have shown in [11], assuming an instantaneous last scattering, i.e. that E modes were produce first and subsequently rotated by PMF, results in relatively minor
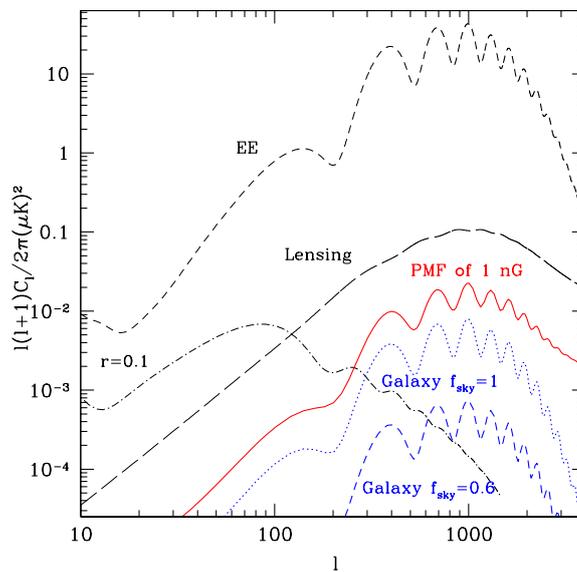
Figure 1. The CMB B-mode spectrum from Faraday rotation sourced at 30 GHz by a scale-invariant primordial magnetic field of 1 nG strength (red solid), by the full sky galactic magnetic field (blue dot), and by the galactic field with Planck's sky mask ($f_{sky} = 0.6$). The black short-dash line is the input E-mode spectrum, the black dash-dot line is the contribution from inflationary gravitational waves with $r = 0.1$, while the black long-dash line is the expected contribution from gravitational lensing by large scale structure.

inaccuracies. In this approximation, the relation between the spherical expansion coefficients of the E, B and α fields can be written as

$$B_{lm} = \sum_{LM} \sum_{l_1 m_1} \alpha_{LM} E_{l_1 m_1} \mathcal{M}_{l_1 m_1}^{LM} \ , \tag{5}$$

where $\mathcal{M}_{l_1 m_1}^{LM}$ is defined in terms Wigner 3-j symbols [21]. We note that B modes from WL can also be schematically written as (5) but with a different mixing matrix $\mathcal{M}_{l_1 m_1}^{LM}$. Importantly, the mixing matrix for WL has a parity opposite to that of FR so that the two rotations are orthogonal to each other, making it possible to reconstruct them separately.

In Fig. 1 we show the B-mode auto-correlation spectra due to FR by a scale-invariant stochastic magnetic fields of 1 nG strength. Also shown is the contribution from FR by the galactic MF, the E mode auto-correlation spectrum which acts as a source for the FR B modes, as well as B modes from inflationary gravitational waves with $r = 0.1$, and the expected contribution from WL.

The FR induced B mode spectra have certain characteristic features. In the case of the nearly scale invariant magnetic spectrum, the spectrum is oscillatory. In fact, the shape of the B-mode spectrum mimics that of the E-mode, except for the lack of exponential damping on small scales. This is because E modes are suppressed by the Silk damping, while PMF can remain correlated on small scales. The damping of the FR induced B-mode power is due to averaging over many random rotations along the line of sight. This translates into a $1/l$ suppression of the angular spectrum, i.e. asymptotically we have $l^2 C_l^{BB} \propto l^{2n-1}$ at large l.

Name - freq (GHz)	$f_{\rm sky}$ $(f_{\rm sky}^{\rm opt})$	FWHM (arcmin)	$\Delta_P(\mu{\rm K\text{-}arcmin})$	$B_{\rm eff}$ $(2\sigma, {\rm nG})$
Planck LFI - 30	0.6	33	240	16
Planck HFI - 100	0.7	9.7	106	23
Polarbear - 90	0.024^a	6.7	7.6	3.3 (3.0)
QUIET II - 40	0.04^a	23	1.7	0.46 (0.26)(0.25)
CMBPOL - 30	0.6	26	19	0.56 (0.55)(0.51)
CMBPOL - 45	0.7	17	8.25	0.38 (0.35)(0.29)
CMBPOL - 70	0.7	11	4.23	0.39 (0.32)(0.26)
CMBPOL - 100	0.7	8	3.22	0.52 (0.4)(0.34)
Suborbital - 30	0.1	1.3	3	0.09 (0.07)(0.05)
Suborbital - 90	0.1	1.3	3	0.63 (0.45)
Space - 30	0.6 (0.2)	4	1.4	0.06 (0.04)(0.02)
Space - 90	0.7 (0.4)	4	1.4	0.26 (0.15)(0.12)

Table 1. The expected 2σ bound in nano-Gauss on the strength of a scale-invariant PMF. The numbers in the first parenthesis are for the case when 99% of the lensing contribution to the B-mode spectrum is subtracted, while the number the in the second parenthesis is after the addition subtraction of the 90% of the galactic FR contribution. Note that for full sky experiments there is an optimal sky cut ($f_{\rm sky}^{\rm opt}$) that gives the best bounds on the PMF. (^{a} based on 0.1 of RM sky)

3. Detectability of the primordial magnetic field

Spatially dependent FR produces additional non-Gaussian signatures in the CMB polarization. Namely, a particular realization of the FR distortion field correlates the respective Legendre coefficients E_{lm} and $B_{l'm'}$. In fact, as shown in [21], it is possible to reconstruct the distortion field $\alpha(\hat{\mathbf{n}})$ from specially constructed linear combinations of products $E_{lm}B_{l'm'}$. The additional correlations induced by FR also manifest themselves as connected 4-point functions of the CMB, which, in turn, provide a measurement of the distortion spectrum $C_L^{\alpha\alpha}$ [22, 23]. In principle, one can construct four estimators of the distortion spectrum, based on products of two CMB fields one of which contains polarization: TE, EE, TB, and EB. Of these four, the first two receive a large contribution to their variance from the usual scalar adiabatic Gaussian perturbations which makes it harder to find the FR signal. In [12, 13, 14], we studied the last two, i.e we considered estimators based on 4-point correlations $\langle EBEB \rangle$ and $\langle TBTB \rangle$. We have fully accounted for the contamination by weak lensing, which contributes to the variance, but whose contribution to the 4-point correlations is orthogonal to that of FR. We also account for the RM from our own galaxy, using the map provide by [29].

We will consider several sets of experimental parameters corresponding to ongoing, future and hypothetical experiments. Namely, we consider Planck's 30 GHz LFI and 100 GHz HFI channels based on actual performance characteristics [24], POLARBEAR [25] at 90 GHz with parameters compiled in [26], QUIET Phase II [27] at 40 GHz using the parameters compiled in [26], 30, 45, 70 and 100 GHz channels of a proposed CMBPol satellite [28], as well as an optimistic hypothetical sub-orbital and space-based experiments at 30 and 90 GHz. The assumed sky coverage ($f_{\rm sky}$), resolution ($\Theta_{\rm FWHM}$), and instrumental noise (Δ_P) parameters are listed in Table 1.

In Table 1 we present our forecasts for 2σ bounds on $B_{\rm eff}$ that can be expected from various ongoing and future CMB experiments. For each experiment, we check the effect of de-lensing as well as further partial subtraction of the galactic rotation measure. The optimal sky cuts are indicated when relevant. One of the interesting facts one can extract from this table is that very competitive bounds can be placed by POLARBEAR and QUIET, while even $\mathcal{O}(10^{-11}{\rm G})$ fields can be constrained in principle by future experiments.
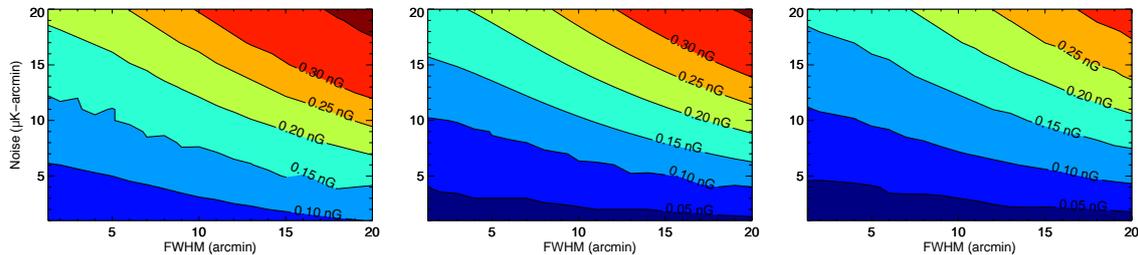
Figure 2. Contour plots of the 2σ bound on B_{eff} (in nG) in the instrumental noise – CMB resolution plane, with the frequency channel taken to be 30 GHz. The left panel shows the case with no de-lensing and without subtracting the Milky Way RM. The middle panel is with de-lensing, while the right panel is with de-lensing and with subtraction of the galactic FR. It is assumed that up to 0.6 of the sky is available and an optimal sky cut is found in each case.

To show the dependence of the PMF bound on the instrumental noise and resolution, we plot contours of constant 2σ bounds on B_{eff} in Fig. 2. The three panels show the cases with and without de-lensing and with an additional partial subtraction of the galactic RM. An optimal sky cut was used for each set of parameters.

4. Summary
We have studied the detectability of a scale-invariant PMF due to FR of the CMB using polarization correlators. We have found that the galactic RM is not a serious barrier to observe a scale-invariant PMF and that the EB quadratic correlator is in general more powerful than the BB correlator.

We have also studied the detectability of the PMF as a function of the sky coverage. We find that suborbital experiments can be almost as effective as space borne experiments, and the obstruction caused by the galaxy is relatively weak if the observed patch is near the poles. Also, as the mode-coupling correlations of CMB are mostly sourced by the largest scale features (low L) of the rotation measure, a full sky CMB map is not necessary to access the PMF on the largest scales. Cross-correlating polarization maps at multiple frequencies with comparable sensitivity to FR can further boost the significance of detection [14].

[1] L. M. Widrow, Rev. Mod. Phys. **74**, 775 (2002) [astro-ph/0207240].
[2] A. Neronov and I. Vovk, Science **328**, 73 (2010) [arXiv:1006.3504 [astro-ph.HE]].
[3] D. Grasso and H. R. Rubinstein, Phys. Rept. **348**, 163 (2001) [astro-ph/0009061].
[4] T. Vachaspati, Phys. Lett. B **265**, 258 (1991).
[5] J. M. Cornwall, Phys. Rev. D **56**, 6146 (1997) [hep-th/9704022].
[6] M. S. Turner and L. M. Widrow, Phys. Rev. D **37**, 2743 (1988).
[7] B. Ratra, Astrophys. J. **391**, L1 (1992).
[8] T. Vachaspati, Phys. Rev. Lett. **87**, 251302 (2001) [astro-ph/0101261].
[9] K. Jedamzik and T. Abel, arXiv:1108.2517 [astro-ph.CO].

[10] A. Kosowsky, T. Kahniashvili, G. Lavrelashvili and B. Ratra, Phys. Rev. D **71**, 043006 (2005) [astro-ph/0409767].

[11] L. Pogosian, A. P. S. Yadav, Y. -F. Ng and T. Vachaspati, Phys. Rev. D **84**, 043530 (2011) [Erratum-ibid. D **84**, 089903 (2011)] [arXiv:1106.1438 [astro-ph.CO]].

[12] A. P. S. Yadav, L. Pogosian and T. Vachaspati, arXiv:1207.3356 [astro-ph.CO].

[13] S. De, L. Pogosian and T. Vachaspati, Phys. Rev. D **88**, 063527 (2013) [arXiv:1305.7225 [astro-ph.CO]].

[14] L. Pogosian, arXiv:1311.2926 [astro-ph.CO].

[15] M. Kamionkowski, A. Kosowsky and A. Stebbins, Phys. Rev. Lett. **78**, 2058 (1997) [astro-ph/9609132].

[16] U. Seljak and M. Zaldarriaga, Phys. Rev. Lett. **78**, 2054 (1997) [astro-ph/9609169].

[17] U. Seljak, U. -L. Pen and N. Turok, Phys. Rev. Lett. **79**, 1615 (1997) [astro-ph/9704231].

[18] T. R. Seshadri and K. Subramanian, Phys. Rev. Lett. **87**, 101301 (2001) [astro-ph/0012056].

[19] K. Jedamzik, V. Katalinic and A. V. Olinto, Phys. Rev. D **57**, 3264 (1998) [astro-ph/9606080].

[20] K. Subramanian and J. D. Barrow, Phys. Rev. D **58**, 083502 (1998) [astro-ph/9712083].

[21] M. Kamionkowski, Phys. Rev. Lett. **102**, 111302 (2009) [arXiv:0810.1286 [astro-ph]].

[22] A. P. S. Yadav, R. Biswas, 1, M. Su and M. Zaldarriaga, Phys. Rev. D **79**, 123009 (2009) [arXiv:0902.4466 [astro-ph.CO]].

[23] V. Gluscevic, M. Kamionkowski and A. Cooray, Phys. Rev. D **80**, 023510 (2009) [arXiv:0905.1687 [astro-ph.CO]].

[24] P. A. R. Ade et al. [Planck Collaboration], arXiv:1303.5062 [astro-ph.CO].

[25] B. Keating, S. Moyerman, D. Boettger, J. Edwards, G. Fuller, F. Matsuda, N. Miller and H. Paar et al., arXiv:1110.2101 [astro-ph.CO].

[26] Y. -Z. Ma, W. Zhao and M. L. Brown, JCAP **1010**, 007 (2010) [arXiv:1007.2396 [astro-ph.CO]].

[27] D. Samtleben [QUIET Collaboration], Nuovo Cim. B **122**, 1353 (2007) [arXiv:0802.2657 [astro-ph]].

[28] D. Baumann et al. [CMBPol Study Team Collaboration], AIP Conf. Proc. **1141**, 10 (2009) [arXiv:0811.3919 [astro-ph]].

[29] N. Oppermann, H. Junklewitz, G. Robbers, M. R. Bell, T. A. Ensslin, A. Bonafede, R. Braun and J. C. Brown et al., arXiv:1111.6186 [astro-ph.GA].